"Al/stainless-invar composites with tailored anisotropy for thermal management in light weight electronic packaging"

Ryelandt, Sophie ; Mertens, Anne ; Delannay, Francis

Abstract

Composite plates in which the low CTE phase has the shape of a honeycomb are anticipated to present optimum anisotropy of thermal expansion and thermal conductivity for baseplates in electronic packaging. This design is explored by choosing an invar alloy for the low CTE phase. In order to allow the formation of a passivation layer protecting from reaction with liquid Al during squeeze casting, the honeycomb is made of the Cr-rich alloy commonly called “stainless-invar”. Composite plates containing 20 vol.% and 38 vol.% stainless invar were processed using honeycombs with the same thickness over cell side ratio. Experimental CTE values are significantly lower than the predictions of three different thermo-elastic models. The very limited amplitude of the strain hysteresis precludes the occurrence of global plastic yielding in the matrix. It appears that, owing to the high contiguity of the lowCTE phase, the lowvalue of the experimental CTE results fromvoid closing and opening by ...

Document type : *Article de périodique (Journal article)*

Materials and Design 85 (2015) 318–323

Contents lists available at ScienceDirect

Materials and Design

journal homepage: www.elsevier.com/locate/jmad

Al/stainless-invar composites with tailored anisotropy for thermal management in light weight electronic packaging

Sophie Ryelandt [a], Anne Mertens [b], Francis Delannay [a,*]

[a] Université catholique de Louvain, Institute of Mechanics, Materials and Civil Engineering, IMAP, Place Ste Barbe, 2, B1348 Louvain-la-Neuve, Belgique
[b] Université de Liège, Faculty of Applied Sciences, A&M Department, Metallic Materials Science Unit, Chemin des Chevreuils, 1 B52/3, B 4000 Liège, Belgique

ARTICLE INFO

Article history:
Received 5 March 2015
Received in revised form 29 June 2015
Accepted 30 June 2015
Available online 6 July 2015

Keywords:
Metal matrix composites (MMCs)
Interface
Thermomechanical properties
Anisotropy
Squeeze casting

ABSTRACT

Composite plates in which the low CTE phase has the shape of a honeycomb are anticipated to present optimum anisotropy of thermal expansion and thermal conductivity for baseplates in electronic packaging. This design is explored by choosing an invar alloy for the low CTE phase. In order to allow the formation of a passivation layer protecting from reaction with liquid Al during squeeze casting, the honeycomb is made of the Cr-rich alloy commonly called "stainless-invar". Composite plates containing 20 vol.% and 38 vol.% stainless invar were processed using honeycombs with the same thickness over cell side ratio. Experimental CTE values are significantly lower than the predictions of three different thermo-elastic models. The very limited amplitude of the strain hysteresis precludes the occurrence of global plastic yielding in the matrix. It appears that, owing to the high contiguity of the low CTE phase, the low value of the experimental CTE results from void closing and opening by localised plastic flow. A honeycomb volume fraction of 38% is necessary for bringing the average CTE down to the level suitable for packaging applications. The ratio of transverse thermal conductivity to density then amounts to about half of the performance of the best Al/SiC composites.

1. Introduction

Current development in electronics leads to a continuous size reduction of the devices which brings about a drastic increase of the heat to be dissipated per unit volume of hardware. Electronic components are attached, directly or via an electrical insulator substrate, on the baseplate of the housing. A major function of the baseplate is the transfer of the heat toward an external heat sink. Thermal stresses are proportional to the mismatch between the linear coefficient of thermal expansion (CTE) of the baseplate and the CTE of the device (~4×10^{-6}/K for Si, ~ 6×10^{-6}/K for GaAs) and/or of the substrate interlayer (4 to 8×10^{-6}/K for Al_2O_3 or AlN) [1]. It follows that, typically between −20 °C and 150 °C, the baseplate material must present both a high thermal conductivity (>100 W/m∗K) and a low CTE (<10^{-5}/K). The housing must resist loads and must be hermetically sealed. The baseplate material should thus also have sufficient strength and ductility, and should be compatible for plating and for assemblage with the other materials of the housing. Obviously, low specific mass is a major additional requirement for mobile electronics.

Today, packaging technology privileges the choice either of Cu–W and Cu–Mo composites, or of low CTE alloys such as Invar® (Fe–Ni36, CTE < 2×10^{-6}/K), N42 (Fe–Ni42, CTE ~ 4.5×10^{-6}/K), and Kovar® (Fe–Ni29–Co17, CTE ~ 5×10^{-6}/K) (we will collectively designate this family of low CTE alloy as "invar") [2]. The high density of these materials is a drawback for aerospace and mobile applications. In addition, the thermal conductivity of invar alloys is low (15 W/m∗K).

Owing to the high thermal conductivity and low density of aluminium alloys, Al-matrix composites are attractive candidates for the baseplate in mobile electronics. All factors that can contribute to the strengthening of an Al-based alloy – reduction of grain size, presence of solute elements and precipitates, strain hardening – bring about a decrease of thermal conductivity. A sufficiently high thermal conductivity can thus be obtained only with a relatively soft matrix alloy. As a corollary, the second phase has to contribute significantly to the strength of the composite. Many types of fibre or particulate have been tested for reinforcing an Al-matrix in view of packaging applications: SiC [3–7], Al_2O_3 [8,9], diamond [10–12], graphite flakes [13], fly ash [14], and carbon nanotubes [15,16]. The composites can be processed by squeeze casting or by powder metallurgy provided to control properly the phenomena governing wetting and interfacial reactions with Al. Common drawbacks are high material and/or fabrication cost and poor suitability of the composites to machining and joining. Today, composites Al/SiC with 40 to 65 vol.% SiC particulates are commercially available for electronics packaging applications.

Potentially, a metal-reinforced composite could offer a better machinability and a better suitability for assemblage of the baseplate with the other parts of the housing. Nevertheless, the most stringent constraint for light weight applications is the tailoring of an adequate

* Corresponding author.
E-mail addresses: sophie.ryelandt@uclouvain.be (S. Ryelandt), anne.mertens@ulg.ac.be (A. Mertens), francis.delannay@uclouvain.be (F. Delannay).

http://dx.doi.org/10.1016/j.matdes.2015.06.178
0264-1275/

compromise between density, ρ, CTE, α, and thermal conductivity, κ. Whereas ρ is a scalar, α and κ are rank-2 tensors. The issue is schematically represented in Fig. 1 (adapted from [17]) which compares, on a chart κ/ρ versus α, the property ranges that should be achievable with composites Al/SiC and composites Al/invar with the same soft Al-base alloy matrix. The Al/invar composite is the novel solution assessed in the present paper. The continuous curves represent upper and lower bounds for the properties of the two composites. These bounds enclose the possible values of the diagonal components of tensors α and κ in all directions. On the graph, the best material for light weight packaging should be located as high as possible and as close as possible to the left hand side. Owing to the higher density and lower thermal conductivity of invar, it is anticipated that a similar κ/ρ ratio could be achieved for composites Al/invar and Al/SiC only if the volume fraction of invar is lower. Ellipses have been drawn to circumscribe the property domains that may be anticipated for a composite Al/65 vol.% SiC and for two composites Al/20 vol.% invar and Al/40 vol.% invar. The ellipses are drawn narrow in the vertical direction because the Al matrix is supposed to present a high contiguity in order to favour thermal conductivity. The properties of isotropic particulate-reinforced composites would be located close to the centre of gravity of the ellipse: typically, the CTE of a commercial composite Al/65 vol.% SiC is close to $8.5\times10^{-6}\,K^{-1}$ (e.g. [18]).

Fig. 1 suggests that, provided the tailoring of the proper anisotropy of reinforcement architecture, a composite Al/20 vol.% invar can be a substitute for Al/SiC composites. A composite Al/40 vol.% invar could also be suitable if the penalty of lower κ/ρ is acceptable. The formability of the metal makes the tailoring of reinforcement architecture much easier than with ceramic. Optimisation requires the coupling of a minimum of the diagonal component of tensor α in the direction parallel to the plate and a maximum of the diagonal component of tensor κ in the direction perpendicular to the plate. It is well documented that the thermal expansion of a composite can be lowered by increasing the contiguity of the low CTE phase [3,8,19–22]. On the other hand, as the thermal conductivity of the metal matrix is primarily due to electron flow, composite thermal conductivity increases when decreasing the scattering of electrons at matrix/reinforcement interfaces [4,17,22,23]. Hence, the best architecture should be such that the invar phase presents a high contiguity parallel to the plane while the Al phase presents a high contiguity perpendicular to the plane. A priori, these conditions would be met by designing composite baseplates in which the invar phase has the shape of a honeycomb. The objective of this paper is to explore that design. The processing conditions of the composite plates are detailed in Section 2, with emphasis on the choice of the invar alloy and on squeeze casting conditions. Section 3 analyses the influence of the invar volume fraction on the thermo-mechanical properties of the composite plates. It is shown that a CTE suitable for the targeted packaging application can be obtained when the invar honeycomb represents 38% of the volume.

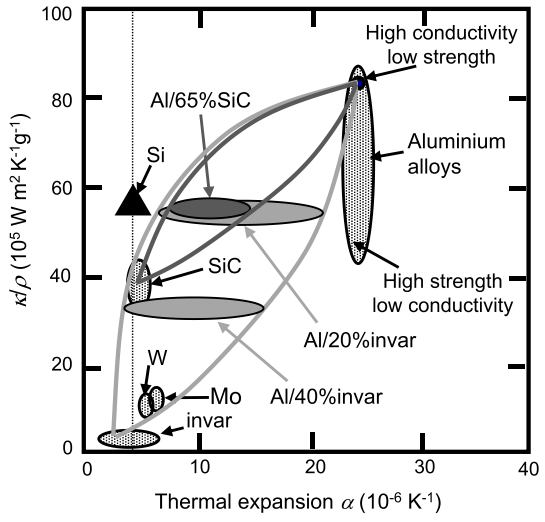

Fig. 1. Schematic chart showing the coupling of thermal conductivity per unit mass, κ/ρ, and thermal expansion, α, for candidate materials for baseplate in electronics packaging (adapted from [17]). The property domains achievable with composites Al/SiC and Al/invar are delineated by upper and lower boundary curves.

2. Materials processing and testing methods

The preparation of metallic composites with invar as second phase has been investigated for Cu matrix composites [24] but never for Al matrix composites. The only feasible route for preparing near-net shape plates of Al-matrix composite reinforced with a honeycomb structure is by infiltrating the honeycomb with liquid Al alloy using a technique such as squeeze casting. However, a major problem arises from the fact that commonly used invar alloys (Invar®, N42, Kovar®) contain essentially Fe and Ni, which are known to strongly react with liquid Al. This reactivity brings about the formation of brittle intermetallic compounds at the matrix/reinforcement interface, which has long prevented the use of Ni-based and Fe-based particles or fibres in Al composites [25,26]. The large exothermic character of the reaction can cause the melting of the reinforcing phase during squeeze casting. This has brought researchers to propose reactive infiltration of liquid Al into the porosity of a Fe- or Ni-based solid skeleton as a method for processing bulk aluminide materials [27–30].

Nevertheless, previous work has shown that sound Al composites reinforced with Fe- or Ni-base fibres can be processed when the fibre alloy contains a high enough concentration of Cr as to make possible the formation of a Cr-rich passivation barrier onto the surface [31–33]. The thickness of the passivation barrier can be varied by heat treatment of the fibres in air before squeeze casting [34,35]. The kinetics of decomposition of this passivation layer can be controlled by tuning the solidification rate during squeeze casting [31].

A Cr-rich invar alloy has been reported in literature, with composition 54% Co, 36.5% Fe and 9.5% Cr [36–38]. This alloy has been denominated “stainless-invar”. In all invar alloys, the occurrence of the invar effect necessitates the stabilisation of the γ (FCC) structure close to room temperature. Carbon being a potent austenite stabilizer, it has been shown that, in the case of stainless-invar, a C content higher than 0.06 wt.% is necessary for having the γ (FCC) structure to be the major constituent. Increasing the carbon content from 0.06 to 0.18 wt.% causes a progressive CTE increase from a minimum close to 2×10^{-6}/K up to about 4.5×10^{-6}/K [39].

An ingot with target composition 53–55 wt.% Co, 36–37 wt.% Fe, 8.5–9.5 wt.% Cr, 0.08 wt.% C was cast from the melt, homogenised at 800 °C for 48 h under Ar, and furnace cooled. The ingot was hot and cold rolled, with two intermediary annealing steps of 10 min at 1000 °C, to produce sheets of 0.6 mm thickness. Notched strips with two different widths $h = 5.1$ mm and $h = 3.0$ mm were machined into the sheets by spark erosion (Fig. 2a). Honeycombs were fabricated by assembling these strips to form grids with square cells (Fig. 2b). For obtaining in-plane isotropy, an alternative could have been to fabricate the honeycombs by assembling the strips into a 2D Kagome structure [40]. Nevertheless, a square-celled architecture was easier to fabricate and was judged sufficient for the purpose of validating the concept. Two honeycombs were fabricated: a honeycomb with volume fraction $V_{invar} = 0.20$, i.e. with a cell size $d = 5.7$ mm, and a honeycomb with $V_{invar} = 0.38$, i.e. $d = 2.8$ mm. The composite plate thickness (i.e. the height of the honeycomb) was $h = 5.1$ mm and $h = 3.0$ mm, respectively, in order to obtain a similar cell aspect ratio $h/d \approx 1$ (optimisation of cell aspect ratio is not investigated in the present work).

The composites were produced by squeeze casting with alloy A1100 at 850 °C using processing set up and conditions that have been detailed in previous work [31,32]. The honeycomb occupied only

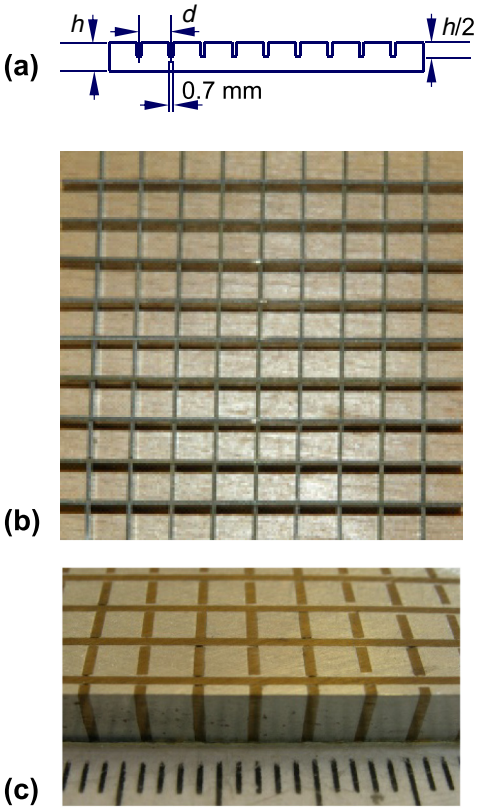

Fig. 2. (a) Drawing of the notched strips used to fabricate the honeycombs. (b) Honeycomb with $V_{invar} = 0.20$. (c) Composite plate with $V_{invar} = 0.38$.

part of the mould in such a way that the shrinkage cavity could localise outside the volume of the composite plates. Prior to casting the liquid metal, the honeycomb had been preheated in air at 350 °C during 1 h for creating the passivation barrier suitable for hindering reaction with liquid Al. This preheating treatment had previously been optimised by tests carried out by dipping sheets of stainless invar in liquid A1100. The plates were machined from the as-cast moulding by milling (Fig. 2c). Observation of the plates by optical microscopy and scanning electron microscopy (SEM) did not reveal the presence of voids inside the matrix.

Thermal expansion was investigated by push rod dilatometry. For the stainless-invar honeycombs and the composite plates, the tests were made on parallelepiped specimens with dimensions 12 × 26 mm aligned along cell sides. CTE evolution with temperature was derived from the raw data of strain evolution with temperature. Unless otherwise specified, the tests were carried out at a rate of 1 K/min. They always involved several consecutive heating-cooling cycles between room temperature (RT) and a maximum of typically 160 °C. Indeed, owing to the redistribution of internal stresses between the matrix and the second phase during the first cycle, reproducible thermal strains were recorded during successive cycles only after the end of the first cycle. Hence, the experimental results presented in this paper are results measured during the second – or a subsequent – heating or cooling ramp.

Thermal conductivity, κ, derives from thermal diffusivity, δ, heat capacity per unit mass, C_p, and mass per unit volume, ρ, according to Laplace's equation,

$$\kappa = \delta \rho C_p. \quad (1)$$

Diffusivity in the direction perpendicular to the composite plate was measured at 40 °C using the laser flash method. C_p was measured by differential scanning calorimetry.

3. Results and discussion

First, the resistance to thermal fatigue was assessed by submitting the composite with 38 vol.% invar to a test involving 12 successive cycles of heating and cooling at 2 K/min between room temperature and 140 °C. The strain curves remained remarkably reproducible after the first cycle: the strain difference between the beginning of the 2nd cycle and the end of the 12th cycle amounted to only $\Delta\varepsilon \approx 0.5 \times 10^{-4}$. Fig. 3 presents a SEM micrograph of the surface of the composite at the end of the 12 cycles. It shows that the preheating treatment of the honeycomb has created, on the surface stainless invar, a strongly adherent, continuous passivation layer of thickness ≈0.25 μm. This layer appears very effective in preventing reaction between Al and stainless invar during squeeze casting [31–33]. However, the corollary of this weak reactivity is a weak interface adhesion: the micrograph shows that thermal cycling has caused some amount of decohesion along the interface between the Al matrix and the passivation layer. The volume fraction of voids due to this decohesion cannot be quantified because it is expected that the apparent opening of the interfacial cracks is affected by the polishing of the sample. The authors believe that, as shown by Salmon et al. [33,35], this interface adhesion could potentially be improved via heat treatment of the composite after squeeze casting.

For both composites, the strain curves recorded during thermal cycling presented a very small strain hysteresis – amounting to less than 1×10^{-4} – between heating and cooling curves. Assuming in-plane isostrain in the two phases, this hysteresis translates into a hysteresis of only $\Delta\sigma < 7$ MPa for the volume average of the in-plane stresses in the Al matrix. The amplitude of this stress hysteresis is a measure of the volume average of the stresses needed to drive inelastic strains during thermal cycling [19]. It may thus be concluded that strains remain purely elastic in the major part of the matrix volume.

Figs. 4 and 5 show the temperature dependence of the in-plane CTE of the composite plates with 20 vol.% and 38 vol.% of stainless-invar, respectively, together with the temperature dependence of the CTE of the matrix Al 1100 and of the stainless-invar honeycomb. The scatter of the points follows from the noise in the raw strain data. Fitting curves have thus been added to highlight qualitatively the trends behind the scatter. The CTE of the composites decreases very drastically with increasing stainless-invar volume fraction. It appears that a volume fraction of 38% is necessary for bringing the average CTE between RT and 150 °C down to a level suitable for packaging applications.

The CTE of the stainless-invar honeycomb increases progressively from 2×10^{-6} at 35 °C to 12×10^{-6} at 150 °C. Such amplitude of increase of the CTE with temperature is commonly observed for the alloys of the invar family. Whereas XRD analysis showed that the structure of the rolled sheets is FCC, with only traces of α (CC) and ε (HCP) phases, chemical analysis revealed a C content somewhat higher than the targeted optimum of 0.08 wt.%. This high C content may have caused a

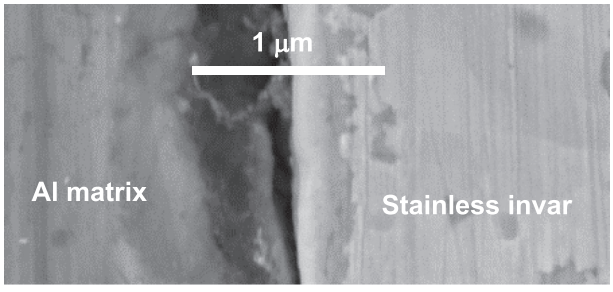

Fig. 3. SEM micrograph of composite Al/38 vol.% stainless-invar after thermal fatigue testing. The surface of stainless invar is covered by a strongly adherent, continuous passivation layer of thickness ≈0.25 mm. Thermal cycling (and sample polishing) has caused the opening of a decohesion crack along the interface between the Al matrix and the passivation layer.

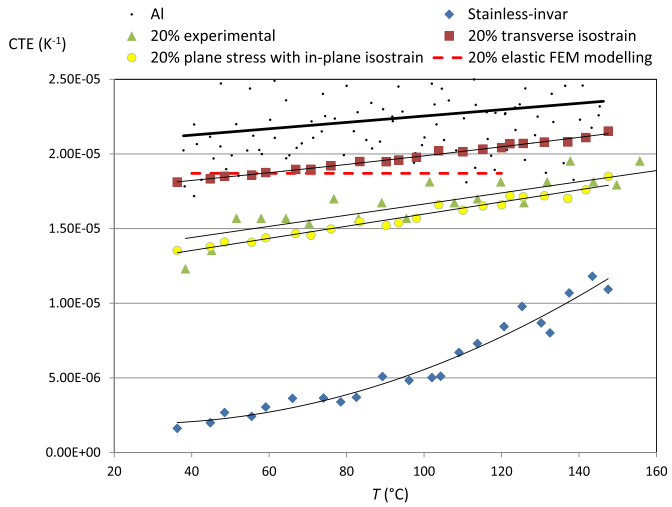

Fig. 4. Temperature dependence of the CTE of the matrix (points), of the stainless-invar honeycomb (diamonds), and of composite plate Al/20 vol.% stainless-invar (triangles), together with predictions of three thermo-elastic models: transverse isostrain (Eq. (2)) (squares); plane stress with in-plane isostrain (Eq. (3)) (circles); FEM computation (dashed horizontal line).

higher CTE than expected [39]. Hence, although the CTE of the honeycomb globally meets the needs of the present work, the authors believe that a fine tuning of the alloy composition could allow further lowering the thermal expansion of the honeycomb in the temperature range targeted for the application.

The CTE of composites is governed in a complex manner by elastic, plastic, and damage phenomena. In order to apprehend the stress state that develops in the phases and the role played by inelastic phenomena, the experimental CTE data presented in Figs. 4 and 5 are compared to the predictions of three different theoretical models that assume pure linear thermo-elasticity.

1. The first model assumes equality of the strain in the two phases in the direction transverse to the plate. This would correspond to the highest possible level of kinematic constraint in the transverse direction, i.e. to an upper bound of the in-plane CTE. This stress state would prevail if the aspect ratio h/d of the honeycomb is large. The in-plane CTE, which we denote $\alpha_{\text{tr·isotrain}}$, is then equal to the CTE in the direction transverse to the fibres for a composite with unidirectional continuous fibres. An approximate expression for this CTE in the framework of isotropic elasticity was proposed by Schapery [41]. An exact solution was derived later by Lu and Hutchinson for transversely isotropic fibres and matrix [42]. Using the non-dimensional coefficients given in [43], if the two phases are isotropic with the same Poisson ratio ν, the solution of Lu and Hutchinson yields [19]:

$$\alpha_{\text{tr·isotrain}} = \alpha_{\text{invar}}V_{\text{invar}} + \alpha_{\text{Al}}V_{\text{Al}} + \nu V_{\text{invar}}V_{\text{Al}}(\alpha_{\text{invar}} - \alpha_{\text{Al}}) \times \frac{E_{\text{Al}} - E_{\text{invar}}}{E_{\text{invar}}V_{\text{invar}} + E_{\text{Al}}V_{\text{Al}}} \frac{\left(\frac{2}{\nu} - 3\right)(E_{\text{invar}}V_{\text{invar}} + E_{\text{Al}}V_{\text{Al}}) - E_{\text{Al}}}{E_{\text{Al}} + (1-2\nu)(E_{\text{invar}}V_{\text{invar}} + E_{\text{Al}}V_{\text{Al}})}. \quad (2)$$

$\alpha_{\text{tr·isotrain}}$ is thus larger than the rule of mixture (ROM) (which is represented by the two first terms in Eq. (2)). Figs. 4 and 5 show, for the two composites, the set of data points calculated according to Eq. (2) using $E_{\text{Al}} = 70$ GPa, $E_{\text{invar}} = 180$ GPa, $\nu = 0.3$ together with the experimental data points for α_{invar} and α_{Al}.

2. The second model assumes plane stress in the two phases in the direction transverse to the plate. This would correspond to the lowest possible level of kinematic constraint in the transverse direction. Phase stresses would progressively tend to plane stress when the aspect ratio h/d of the honeycomb decreases. In addition, this second model assumes the equality of the in-plane strains in the two phases. It can easily be demonstrated that, for two isotropic phases with identical Poisson ratio ν, the in-plane CTE, which we denote, $\alpha_{\text{pl·stress, in-plane isotrain}}$, then expresses as

$$\alpha_{\text{pl·stress in-plane isostrain}} = \alpha_{\text{invar}}V_{\text{invar}} + \alpha_{\text{Al}}V_{\text{Al}} - V_{\text{invar}}V_{\text{Al}}(\alpha_{\text{invar}} - \alpha_{\text{Al}}) \frac{E_{\text{Al}} - E_{\text{invar}}}{E_{\text{invar}}V_{\text{invar}} + E_{\text{Al}}V_{\text{Al}}}. \quad (3)$$

$\alpha_{\text{pl·stress, in-plane·isotrain}}$ is thus lower than the ROM. Expression (3) is identical to the solution of Shapery [41] for the longitudinal CTE of a composite with unidirectional continuous fibres. Figs. 4 and 5 show the set of data points calculated according to Eq. (3) using $E_{\text{Al}} = 70$ GPa, $E_{\text{invar}} = 180$ GPa, $\nu = 0.3$, together with the experimental data points for α_{invar} and α_{Al}.

3. The third modelling approach consists in computing thermo-elastic stresses and strains by 3D FEM simulations on a representative volume element (RVE) with aspect ratio $h/d = 0.87$. ABAQUS® computations were carried out using a single set of material parameters: $E_{\text{Al}} = 70$ GPa, $E_{\text{invar}} = 180$ GPa, $\nu_{\text{Al}} = 0.335$, $\nu_{\text{invar}} = 0.3$, $\alpha_{\text{invar}} = 2 \times 10^{-6}$ (i.e. α_{invar} measured around 40 °C) and $\alpha_{\text{Al}} = 23 \times 10^{-6}$ (i.e. α_{Al} measured around 120 °C). The CTE calculated in this way should thus be merely considered as an approximation for the interval 40–120 °C. It is represented by dashed horizontal lines in Figs. 4 and 5.

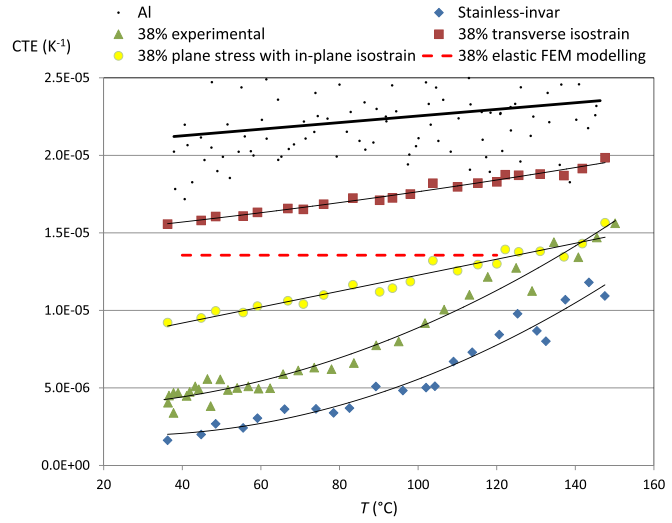

Fig. 5. Temperature dependence of the CTE of the matrix (points), of the stainless-invar honeycomb (diamonds), and of composite plate Al/38 vol.% stainless-invar (triangles), together with predictions of three thermo-elastic models: transverse isostrain (Eq. (2)) (squares); plane stress with in-plane isostrain (Eq. (3)) (circles); FEM computation (dashed horizontal line).

FEM simulations indicate that, in the case of pure elasticity, transverse isostrain would predominate in composite Al/20% invar whereas the stress state in composite Al/38% invar would be intermediate between plane stress and transverse isostrain. This is not unexpected: it is anticipated that the volume average of the strain mismatch between the phases increases when the invar honeycomb volume fraction increases. On the other hand, the experimental CTE is, for both composites, significantly lower than thermo-elastic predictions. For composite Al/20% invar, the experimental CTE corresponds more or less to the prediction assuming plane stress in the transverse direction, which contradicts FEM simulations. For composite Al/38% invar, the low value of the CTE cannot be justified in the framework of pure thermo-elasticity.

As mentioned already, the very small amplitude of the strain hysteresis indicates that the volume average of the stresses driving inelastic

phenomena is very much lower than the yield strength of the matrix. This precludes the occurrence of global plastic yielding in the matrix during thermal cycling. Hence, the discrepancy between experimental results and thermo-elastic predictions must be ascribed to the presence of voids. The essential role that can be played by voids in the expansion behaviour of composites has been much emphasised in the recent literature (see section 5 of ref. [19] for a review). The presence of these voids brings about a relaxation of thermal stresses in the matrix, which causes a reduction of the CTE in composites with high reinforcement contiguity. Even in the purely elastic regime, composites containing voids can present a CTE lower than the lower elastic bound for two-phase composites [44]. More often, low CTE values arise as a result of the closing and opening of voids induced by plastic flow localised around the voids. The influence of the plastic flow localised around voids has been analysed by FEM simulations [20,45] (the RVE model analysed by Shen [20] is very similar to the honeycomb architecture studied in the present work). These simulations demonstrate a drastic decrease of CTE when the contiguity of the low CTE phase is large. For example, Nam et al. [45] show that, in a composite Al/70 vol.% SiC_p, plastic filling of the pores during heating brings a void volume fraction of 0.25 vol.% at RT to be reduced to 0.10 vol.% at 500 °C. A change of the void volume fraction of 0.15 vol.% between heating and cooling is sufficient to justify the departure of the CTE from the prediction of thermo-elastic models [45]. The amplitude of this change is similar to the amplitude of the "non-thermal" volume strain that can be inferred by subtracting the volume expansion the phases from the volume expansion of the composite [19].

As argued by several authors [46,47], in composites prepared by liquid metal infiltration of a 3D-continuous reinforcement, it is unavoidable that, even if infiltration had been perfect, at least 1 vol.% of voids is generated by the hydrostatic tension that arises in the matrix during cooling from the infiltration temperature. Quantification of such a low void volume fraction by metallography is a complex issue. Although hydrostatic tension in the matrix during cooling is lower in the 2D-architectured composites studied in the present work, it cannot be excluded that shrinkage microvoids may be present at the interface already before thermal cycling. Moreover, the micrograph of Fig. 3 indicates that thermal cycling has brought about, close to the surface of the composite plate, the opening of debonding cracks along the interface between the matrix and the passivation layer. These cracks are too small to allow faithful estimation of their volume fraction by SEM metallography (accounting also for the effect of the polishing treatment). Only high resolution x-ray tomography makes possible the direct measurement of void volume fraction and the observation of the occurrence of void closure and re-opening during thermal cycling. This type of experiment has been carried out for the first time by Schöbel et al. [47] on composites Al/60–70 vol.% SiC_p and AlSi7/60–70 vol.% SiC_p thermally cycled in-situ between RT and 400 °C. The composites had been produced by infiltration of densely packed SiC particle preforms. For example, in the AlSi7 matrix composite, the void volume fraction was observed to decrease from 1.7 vol.% to 0.8 vol.% during heating and to increase back to 1.3 vol.% during cooling.

It can thus be concluded that the presence of voids is a condition for bringing the in-plane CTE down to the level required for baseplates in electronic packaging. Obviously, the corollary is that attention needs to be paid to the issue of stability of the voids during thermal cycling. This issue has not been thoroughly explored in this work. At least, it has been observed that composite Al/38% invar exhibits a perfectly stable behaviour during 12 successive heating-cooling cycles between RT and 140 °C.

Owing to the absence of Al/invar interfaces in the direction transverse to the plate, it had been anticipated that the transverse conductivity of the composites would be close to the upper bound expressed by the ROM [13]. This was confirmed by conductivity tests: good agreement with the ROM prediction was obtained within the limits of experimental precision. Taking $\kappa_{Al} = 254\ Wm^{-1}\ K^{-1}$ and $\kappa_{invar} = 15.5\ Wm^{-1}\ K^{-1}$, this yields $\kappa_{transverse} \approx 206\ Wm^{-1}\ K^{-1}$ for the plate with 20 vol.% invar and $\kappa_{transverse} \approx 163\ Wm^{-1}\ K^{-1}$ for the plate with 38 vol.% invar. Accounting for the density the composites, this yields $\kappa/\rho = 54\ Wm^2g^{-1}\ K^{-1}$ and $\kappa/\rho = 33\ Wm^2g^{-1}\ K^{-1}$, respectively. These ratios correspond very well to the values anticipated in Fig. 1. This confirms that, from the point of view of thermal conductivity per unit mass, composite Al/38% invar cannot match the best Al/SiC composites.

4. Conclusions

Al-matrix composites are widely studied for potential application in light-weight electronic packaging. A priori, the best architecture for achieving the optimum anisotropy of thermal expansion and thermal conductivity is a composite plate in which the low CTE phase has the shape of a honeycomb. This work explores this novel design by making use of an invar alloy for the low CTE phase. The outcomes can be summarised as follows.

- In order to allow control of the reactivity between the liquid matrix and the honeycomb during squeeze casting, use has to be made of an alloy containing a high enough Cr content to make possible the formation of a protective passivation layer. This condition can be fulfilled with alloy "stainless-invar", with composition 53–55 wt.% Co, 36–37 wt.% Fe, 8.5–9.5 wt.% Cr, 0.08 wt.% C.
- Composite plates have been processed using stainless-invar honeycombs consisting of 20 vol.% invar and 38 vol.% invar with the same cell aspect ratio, which were fabricated from rolled sheets of 0.6 mm thickness. The plates exhibit very limited strain hysteresis during thermal cycling between RT and 150 °C, which precludes the occurrence of global plastic yielding in the matrix. Microscopic observation shows that thermal stresses bring about the opening of decohesion cracks along the interface between the Al matrix and the passivation layer.
- Experimental CTE values are significantly lower than the predictions of three different thermo-elastic models used to apprehend the stress state in the phases during heating and cooling. This allows concluding that, as the contiguity of the invar phase is high, the CTE is reduced by localised plastic flow inducing the closure or opening of decohesion voids at interfaces.
- A honeycomb volume fraction of 38% is necessary for bringing the average CTE down to the level suitable for electronic packaging applications. For this volume fraction, the ratio of the transverse thermal conductivity to the density is about 33 $Wm^2g^{-1}\ K^{-1}$.
- Potentially, the performance of the composites could still be improved by tuning the composition of the stainless-invar alloy, by improving the stability of interface bonding via heat-treatment, and by optimising the aspect ratio of honeycomb cells.

Acknowledgements

The work was carried out with the support of Walloon Region (Belgium) under contract FIRST 991/3916. The authors gratefully acknowledge the contribution of Fréderic Famularo in the experimental and modelling aspects of this work. They are indebted to Prof. J. Lecomte of University of Liège (ULg, Belgium) for the thermal diffusivity measurements.

References

[1] D.R. Frear, The mechanical behavior of interconnect materials for electronic packaging, JOM (March 1999) 22–27.
[2] Y. Nakamura, Invar systems, Springer Ser. Solid-State Sci. 92 (1991) 111–132.
[3] T. Huber, H.P. Degischer, G. Lefranc, T. Schmitt, Thermal expansion studies on aluminium-matrix composites with different reinforcement architecture of SiC particles, Compos. Sci. Technol. 66 (2006) 2206–2217.
[4] K. Chu, C. Jia, X. Liang, H. Chen, H. Guo, Thermal conductivity of pressure infiltrated SiCp/Al composites with various size distributions: experimental study and modeling, Mater. Des. 30 (2009) 3497–3503.

[5] L. Weber, G. Sinnicco, J.-M. Molina, Influence of processing route on electrical and thermal conductivity of Al/SiC composites with bimodal particle distribution, J. Mater. Sci. 45 (2010) 2203–2209.
[6] J.-M. Lee, S.-K. Lee, S.-J. Hong, Y.-N. Kwon, Microstructures and thermal properties of A356/SiCp composites fabricated by liquid pressing method, Mater. Des. 37 (2012) 313–316.
[7] X.G. Wang, H.Y. Ren, M. Zhu, L.R. Deng, S.H. Lu, The research of β-SiCp/Al electronic packaging composites fabricated by pressureless infiltrating, Adv. Mater. Res. (2012) 3816–3821.
[8] G. Roudini, R. Tavangar, L. Weber, A. Mortensen, Influence of reinforcement contiguity on the thermal expansion of alumina particle reinforced aluminium composites, Int. J. Mater. Res. 101 (2010) 1113–1120.
[9] M.L. Young, R. Rao, J.D. Almer, D.R. Haeffner, J.A. Lewis, D.C. Dunand, Effect of ceramic preform geometry on load partitioning in Al_2O_3–Al composites with three-dimensional periodic architecture, Mater. Sci. Eng. A526 (2009) 190–196.
[10] L. Weber, R. Tavangar, Diamond-based metal matrix composites for thermal management made by liquid metal infiltration — potential and limits, Adv. Mater. Res. 59 (2009) 111–115.
[11] J. Long, X. Li, D. Fang, P. Peng, Q. He, Fabrication of diamond particles reinforced Al-matrix composites by hot-press sintering, Int, J. Refract. Met. Hard Mater. 41 (2013) 85–89.
[12] J.M. Molina-Jordá, Design of composites for thermal management: aluminum reinforced with diamond-containing bimodal particle mixtures, Compos. A: Appl. Sci. Manuf. 70 (2015) 45–51.
[13] J.K. Chen, I.S. Huang, Thermal properties of aluminum-graphite composites by powder metallurgy, Compos. Part B 44 (2013) 698–703.
[14] W.A. Uju, I.N.A. Oguocha, A study of thermal expansion of Al–Mg alloy composites containing fly ash, Mater. Des. 33 (2012) 503–509.
[15] C.F. Deng, Y.X. Ma, P. Zhang, X.X. Zhang, D.Z. Wang, Thermal expansion behaviors of aluminum composite reinforced with carbon nanotubes, Mater. Lett. 62 (15) (May 31, 2008) 2301–2303.
[16] L. Aryasomayajula, K.-J. Wolter, Carbon nanotube composites for electronic packaging applications: a review, J. Nanotechnol (2013) http://dx.doi.org/10.1155/2013/296517 (6 pp.).
[17] H.R. Shercliff, M.F. Ashby, Design with metal matrix composites, Mater. Sci. Technol. 10 (1994) 443–451.
[18] CPS Technologies Corporation, http://www.alsic.com/pdf/data_sheet.pdf June 2015.
[19] F. Delannay, Thermal stresses and thermal expansion in MMCs, in: A. Kelly, C. Zweben (Eds.), Comprehensive Composite Materials, vol. 3, Elsevier Science Ltd., Oxford 2000, pp. 341–369 (chapter 13).
[20] Y.L. Shen, Combined effect of microvoids and phase contiguity on the thermal expansion of metal-ceramic composites, Mater. Sci. Eng. A237 (1997) 102–108.
[21] S. Roy, P. Albrecht, L. Przybilla, K.A. Weidenmann, M. Heilmaier, A. Wanner, Effect of phase architecture on the thermal expansion behavior of interpenetrating metal/ceramic composites, Processing and Properties of Advanced Ceramics and Composites V — Materials Science and Technology 2012 Conference, MS and T 2012. Pittsburgh, PA 2013, pp. 33–43.
[22] S. Li, D. Xiong, M. Liu, S. Bai, X. Zhao, Thermophysical properties of SiC/Al composites with three dimensional interpenetrating network structure, Ceram. Int. 40 (2014) 7539–7544.
[23] C.W. Nan, R. Birringer, D.R. Clarke, H. Gleiter, Effective thermal conductivity of particulate composites with interfacial thermal resistance, J. Appl. Phys. 81 (1997) 6692–6699.
[24] D. Wu, S. Wu, L. Yang, C. Shi, Y. Wu, W. Tang, Preparation of Cu/Invar composites by powder metallurgy, Powder Metall. 58 (2015) 100–105.
[25] R.B. Bhagat, Growth kinetics of interface intermetallic compounds in stainless steel reinforced aluminium matrix composites, J. Mater. Sci. 24 (1989) 1496–1502.
[26] F. Barbier, M.H. Ambroise, In-situ process for producing aluminium matrix composites containing intermetallic material, J. Mater. Sci. Lett. 14 (1995) 457–459.
[27] D.C. Dunand, J.L. Sommer, A. Mortensen, Synthesis of bulk and reinforced nickel aluminides by reactive infiltration, Metall. Trans. A A24 (1993) 2161–2170.
[28] D.C. Dunand, Reactive synthesis of aluminide intermetallics, Mater. Manuf. Process. 10 (1995) 373–403.
[29] J. Lapin, D. Tiberghien, F. Delannay, On the parameters affecting the formation of iron aluminides during pressure-assisted infiltration of aluminium into a preform of steel fibres, Intermetallics 8 (2000) 1429–1438.
[30] D. Tiberghien, J. Lapin, S. Ryelandt, F. Delannay, On the control of the residual porosity in iron aluminides processed by reactive squeeze-infiltration of aluminium into a preform of steel fibres, Mater. Sci. Eng. A 332 (2002) 427–435.
[31] F. Boland, C. Colin, F. Delannay, Control of interfacial reactions during liquid phase processing of aluminium matrix composites reinforced with Inconel 601 fibres, Metall. Mater. Trans. A A29 (1998) 1727–1739.
[32] F. Boland, C. Colin, C. Salmon, F. Delannay, Tensile flow properties of Al-base matrix composites reinforced with a random planar network of continuous metallic fibres, Acta Mater. 46 (1998) 6311–6323.
[33] C. Salmon, C. Colin, R. Molins, F. Delannay, Strengthening of Al/Ni-based composites by in situ growth of intermetallic particles, Mater. Sci. Eng. A 334 (2002) 193–200.
[34] C. Salmon, D. Tiberghien, R. Molins, C. Colin, F. Delannay, Oxidation behaviour in air of thin IN601 fibres, Mater. High Temp. 17 (2000) 271–278.
[35] C. Salmon, D. Tiberghien, R. Molins, C. Colin, F. Delannay, Influence of the oxidation conditions of the fibres on the mechanical properties of Al matrix composites reinforced with Ni-based fibres, Mater. Sci. Forum 369–372 (2001) 435–442.
[36] H. Masumoto, On the thermal expansion of alloys of cobalt, iron, and chromium, and a new alloy, “Stainless-Invar”, Sci. Rep. Tohoku Univ. Ser. 123 (1934) 265.
[37] H. Saito (Ed.), Physics and applications of invar alloys, Honda Materials Series on Materials ScienceMaruzen Company, Tokyo 1978, pp. 3–17.
[38] E.F. Wassermann, in: K.H.J. Buschow, E.P. Wohlfarth (Eds.),Invar: moment-volume instabilities in transition metals and alloys Handbook of Ferromagnetic Materials, vol. 5 1990, pp. 237–322 (North-Holland, Amsterdam).
[39] P. Hidnert, R.K. Kirby, Thermal expansion and phase transformations of low-expanding cobalt–iron–chromium alloys, J. Res. Natl. Bur. Stand. 55 (1955) 29–37.
[40] S. Hyun, S. Torquato, Optimal and manufacturable two-dimensional, Kagome-like cellular solids, J. Mater. Res. 17 (2002) 137.
[41] R.A. Schapery, Thermal expansion coefficients of composite materials based on energy principles, J. Comp. Mater. 2 (1968) 380–404.
[42] T.J. Lu, J.W. Hutchinson, Effect of matrix cracking and interface sliding on the thermal expansion of fibre-reinforced composites, Composites 26 (1995) 403–414.
[43] J.W. Hutchinson, H.M. Jensen, Models of fiber debonding and pullout in brittle composites with friction, Mech. Mater. 9 (1990) 139–163.
[44] O. Sigmund, S. Torquato, Design of materials with extreme thermal expansion using a three-phase topology optimization method, J. Mech. Phys. Solids 45 (1997) 1037–1067.
[45] T.N. Nam, G. Requena, P. Degischer, Thermal expansion behaviour of aluminum matrix composites with densely packed SiC particles, Compos. Part A 39 (2008) 856–865.
[46] S. Elomari, R. Boukhili, C. San Marchi, A. Mortensen, D.J. Lloyd, Thermal expansion responses of pressure infiltrated SiC/Al metal-matrix composites, J. Mater. Sci. 32 (1997) 2131–2140.
[47] M. Schöbel, W. Altendorfer, H.P. Degischer, S. Vaucher, T. Buslaps, M. Di Michiel, M. Hofmann, Internal stresses and voids in SiC particle reinforced aluminum composites for heat sink applications, Compos. Sci. Technol. 71 (2011) 724–733.